Coordinated optimal dispatch of photovoltaic units with updated power electronic transformer

Gao, Shuang; Jia, Hongjie; Yang, Baotong; Liu, Chunhua

Published in:
Energy Procedia

Published: 01/02/2019

Published version (DOI):
10.1016/j.egypro.2019.01.020

Publication details:
Gao, S., Jia, H., Yang, B., & Liu, C. (2019). Coordinated optimal dispatch of photovoltaic units with updated power electronic transformer. *Energy Procedia*, *158*, 6693-6700. https://doi.org/10.1016/j.egypro.2019.01.020

Available online at www.sciencedirect.com

ScienceDirect

Energy Procedia 158 (2019) 6693–6700

Energy Procedia

www.elsevier.com/locate/procedia

10th International Conference on Applied Energy (ICAE2018), 22-25 August 2018, Hong Kong, China

Coordinated optimal dispatch of photovoltaic units with updated power electronic transformer

Shuang Gao[a], Hongjie Jia[a]*, Baotong Yang[a], Chunhua. Liu[b]

[a]School of Electrical and Information Engineering, Tianjin University, Tianjin, China
[b] School of Energy and Environment, City University of Hong Kong, Hong Kong, China

Abstract

The stochastic variation of photovoltaic (PV) generation units in the distribution grid has increased complexity of the optimal dispatch. Updated power electronics devices such as power electronics transformer (PET) are installed to improve the energy efficiency of DC power appliances and the control flexibility. The synergy effects of optimal dispatch of photovoltaic units and updated PET operation are analyzed in this paper. A two-stage optimization model is established to search for the best configuration and operation of distribution grid with updated PET feeders and photovoltaic inverters. The optimal configuration of PETs is given in the upper stage and given to the lower stage as input parameters to regulate the active and reactive power of photovoltaic inverters associated with operation of feeders updated with PETs. The coordinated optimization between updated PETs and photovoltaic generation units is developed to minimize the operation cost and total power losses in the distribution grid. NSGA-II algorithm is adopted to solve the proposed multi-objective optimization with constraints from both reliable operation of power system and power electronics devices. Comparisons between the simulation results with and without the proposed coordinated optimization for PETs and PVs valid the effectiveness of two-stage optimization model. The operation cost and power losses are reduced while avoiding the power curtailment of PV units by optimally configuring and regulating the power electronic devices including the PETs and inverters of PVs in the test distribution network.

Peer-review under responsibility of the scientific committee of ICAE2018 – The 10th International Conference on Applied Energy.

Keywords: integration of photovoltaic generation; coordinated optimal dispatch; multi-objective optimization; power electronic transformer

Peer-review under responsibility of the scientific committee of ICAE2018 – The 10th International Conference on Applied Energy.
10.1016/j.egypro.2019.01.020

1. Introduction

To cope with global energy crisis and environmental pollution, the renewable energy generation resources (RES) are required to be integrated into the power grid. However, the conventional distribution feeders were designed to sustain unidirectional power flows to residential neighborhoods [1-3]. The increased penetration of household renewable energy generation units such as roof-top photovoltaic panel and micro-wind turbine has highlighted pressing needs to address power quality and reliability concerns, especially when RES exceeds the local power demand. A multi-period optimal scheduling with updated power electronic transformer (PET) [4-5] is proposed in this paper to control the large amount of small-scale RES power station and household generation units clustered at the feeders of the medium-voltage (MV) power network, with the objective of maximizing the consumption of RES and ensuring reliability constraints.

Power electronic devices have been widely used in the power system to replace the traditional electric equipment such as switches and transformers in the low-voltage (LV) and mid-voltage (MV) levels. As residential photovoltaic units and electric vehicles are extensively connected to the power network, DC feeders are to be built to facilitate the integration of DC generation units and loads. PETs can be installed to replace the MV/LV transformers to form AC/DC hybrid power distribution system. Dispatching signals can be received by PET to adjust the direction and rate of power flow in the power network to achieve the control objective set by the grid operator. Multiple terminals of PET can be connected to high / low voltage DC feeders and high / low voltage AC feeders. Each terminal can be connected to other feeders of different bus so that a DC or AC link can be built to form new network topology, offering new path for electric power transmission. Compared to the traditional power network (radial or meshed), PETs improve the reliability and flexibility of the distribution grid.

In order to coordinate the optimal dispatching of residential PV inverters and the operation of PETs, the optimal configuration of updated PET feeders and the operation of PV generation units are two sub-problems to be addressed. A two-stage approach is applied to solve the coupled optimal PET configuration and operation of RES in the whole power network. The decision variables in the optimal configuration of updated PET feeders include the size of the PET and the bus to place the traditional MV/LV transformer. Under the configuration of updated PET feeders, the optimal dispatching of PV inverters over the day is implemented, which means that the optimal solution of the first-stage optimization problem is the input of the second-stage optimization of RES active and reactive power. The two optimization sub-problems are performed iteratively until the coupled RES configuration and operational optimization problem is solved. The optimal scheduling model is formed with the objectives of enabling larger integration of distributed RES into residential distribution network without violating the stability of network operation as well as reducing the operation cost and power losses of the distribution network. The discrete variables of optimal RES cluster configuration and continuous decision variables of RES real and active power set points are processed separately in the two sub-problems. The multi-objective optimization problem can be categorized to the quadratic, non-linear constrained optimal power flow (OPF) problem [6-7]. Non-dominated Sorting Genetic Algorithms-II (NSGA-II) is implemented to solve such problem with fast computation speed that can be adopted to practical large-scale RES energy management system.

2. Mathematical model of coordinated control for PV inverters and PET

Power electronics interfaced renewable energy generation units and the transformer can be controlled in the modern distribution grid. The main function of PET is achieved by fully controlled power electronics converters, which is usually formed by cascade H bridge or modular multi-level converter topology. DC generation units such as PV inverter and DC loads can be connected to DC terminals of PET. DC network and AC network can be consequently established to flexibly select the energy path between generation and load with different nature. With the updated PET at MV/LV feeders, the generation units and loads in different DC/AC networks can be connected and the power flow can be controlled according to the capacity and topology of PET. In this paper, the optimal control of power electronic devices is studied in the distribution network with updated PET and PV inverters. In this paper, it is assumed that the traditional MV/LV transformer at certain bus will be replaced by the PET to facilitate the integration of massive residential PV units scattered along the LV feeders, as shown in Fig. 1. Based on this assumption, the controllable PET and PV inverters can be coordinated to achieve the multi-objective optimization to minimize the operating cost and maintain the quality of power supply.

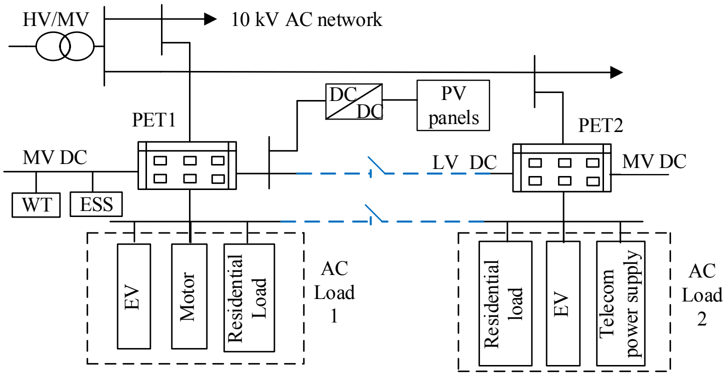

Fig. 1. PET installed in the MV/LV distribution grid with DC/AC generation and loads

2.1. Objective function

The time-series simulation of PET configuration and power regulation of PV inverters considering network constraints is a mixed integer nonlinear programming (MINLP) problem [8-11]. A multi-objective function is formulated to minimize the operating cost and power losses with constraints of voltage deviation in accordance with the standard of power quality in distribution networks. To calculate the cost, the expenditure on supplying electricity to the load considering the operating cost of PV generation units and the total power loss are calculated as in equation (1):

$$f1 = \min \sum_{t=0}^{T} \sum_{i=1}^{n} [\rho_{el}(t)\left(P_{Ld}(t) - P_{Vi}(t) + P_{Ls}(t)\right) + \rho_V(t) P_{Vi}(t)]\Delta t \tag{1}$$

where $\rho_{el}(t)$ is the electricity price at time *t*; $P_{Ld}(t)$ is the net power load of the original distribution system; $\rho_V(t)$ is the operating cost of PV generation; $P_{Vi}(t)$ is the accumulated PV generation power at bus *i*; $P_{Ls}(t)$ is the total power loss at time t; and Δt is the time interval which is one hour as defined in the proposed day-ahead optimal dispatch of PV generation associated with the optimal configuration and control of PETs.

$$f2 = \min \sum_{t=0}^{T} P_{Ls}(t)\Delta t \tag{2}$$

where $P_{Ls}(t)$ is the second objective which can be expressed by:

$$P_{LS}(t) = \sum_{(i,j)\in B} R_{ij} \frac{P_{ij}^2 + Q_{ij}^2}{|V_i|^2} \tag{3}$$

where P_{ij} and Q_{ij} are the active and reactive power transmitted on the branch between bus *i* and *j*; $|V_i|$ is the voltage magnitude at bus *i*, and R_{ij} is the resistance of branch *ij*.

2.2. Constraints

The mathematical model is subject to constraints from several aspects, including power flow equations, reliability of power system operation, and the operating limits on PV inverters and PETs.

$$I_{ij}(t)^2 = \left(G_{ij}^2 + B_{ij}^2\right)\left[U_i^2(t) + U_j^2(t) - 2U_i(t).U_j(t)\cos\theta_{ij}(t)\right] \le I_{ij\max}^2 \tag{4}$$

where $I_{ij}(t)$ is the branch current; G_{ij} and B_{ij} denote admittance matrix of the power network; U_i and U_j are the bus voltage; and $I_{ij\max}$ is the maximum current of transmission line.

$$\left(V_i^{\min}\right)^2 \le V_i^r(t)^2 + V_i^{im}(t)^2 \le \left(V_i^{\max}\right)^2 \tag{5}$$

where $V_i^{\min}$ and $V_i^{\max}$ are the lower and upper limits of bus voltage; $V_i^r(t)$ and $V_i^{im}(t)$ are the real and imaginary parts of the bus voltage.

3. Two-stage multi-objective optimization algorithm

In the proposed coordinated optimization model, the decision variables include the setting of PETs in the upgraded distribution grid with massive DC devices integrated and the power of PV inverters. The increased number of variables makes it even harder to solve the MINLP problem. Thus, a two-stage algorithm is formulated to separate the variables into two categories, which are PET configuration and optimal dispatching of the controllable power of PET and PV inverters. The original problem is converted to a upper-stage time-series optimization and lower-stage power regulation so as to reduce the complexity of the nonlinear constrained optimization modeled in the above section.

3.1. Solution procedure

A two-stage multi-objective optimization algorithm based on NSGA-II is derived to provide a viable solution to the complex MINLP problem described in the above section, as depicted in Fig. 2. As shown in the flowchart, the problem solution of the two-stage optimization algorithm requires an iterative process between the upper-stage optimization of PET configuration and the lower-stage optimization of power regulation for the controllable power electronic devices. In the upper stage, the optimal locations of PETs are found and are sent to lower-stage optimization as input parameters. Power regulation of PET terminals and PV inverters is implemented at each time interval due to the time-independent nature of the lower-stage optimization problem.

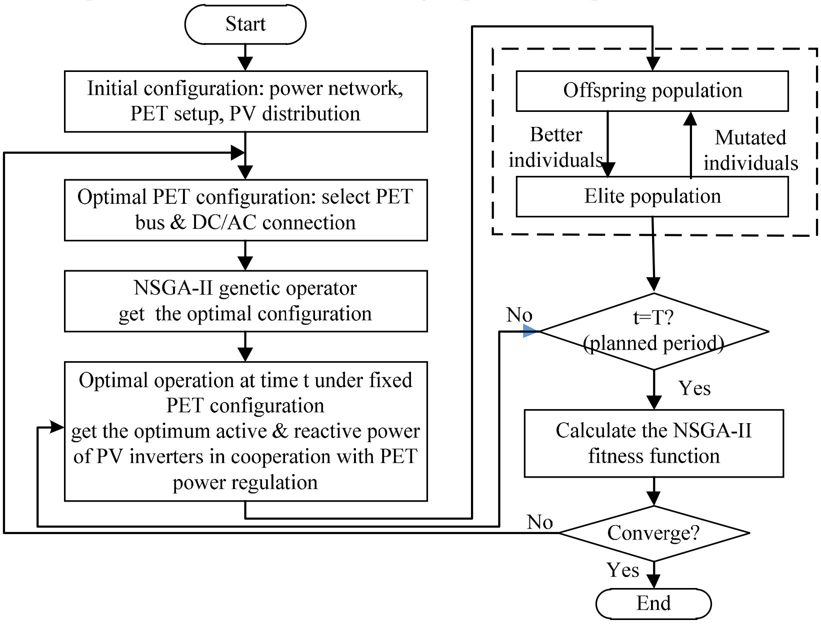

Fig 2. Flowchart of the proposed coordinated optimization algorithm

3.2. Mathematical formulation of coupled upper and lower optimization stages

The overall objective is described in equation (1) with the PET configuration and power regulation as decision variables and subject to:

$$P_{i,PET}^{ACH}(t)+P_{i,PET}^{ACL}(t)+P_{i,PET}^{DCH}(t)+P_{i,PET}^{DCL}(t)+P_{i,PET}^{LS}(t)=0 \tag{6}$$

where $P_{i,PET}^{ACH}(t)$ and $P_{i,PET}^{ACL}(t)$ are the power flow of the two AC terminals of the PET; $P_{i,PET}^{DCH}(t)$ and $P_{i,PET}^{DCL}(t)$ are the power flow of the high-voltage DC terminal and low-voltage DC terminal; and $P_{i,PET}^{LS}(t)$ denotes the power loss of the PET at bus *i*.

$$P_{i,PET}^{ACH}(t)-P_{i,Ld}^{ACL}(t)+P_{i,PV}^{DC}(t)=P_{j,Ld}^{ACL}+P_{j,Ld}^{DC}(t)-P_{j,PET}^{ACH}(t) \tag{7}$$

where $P_{i,Ld}^{ACL}(t)$ is the power load connected to low-voltage AC terminal of PET at bus *i*; $P_{i,PV}^{DC}(t)$ is the PV generation connected to DC terminal; $P_{j,Ld}^{ACL}$ and $P_{j,Ld}^{DC}(t)$ are the power loads connected to the low-voltage AC terminal and DC terminal of PET at bus *j*.

$$LC_{i,\ PET}\in\{0,1\} \tag{8}$$

where $LC_{i,PET}$ represents if PET is located at bus *i*, and in this algorithm is defined as binary variable.

$$N_A^{\min}\le\sum_{i=1}^{n}LC_{i,\ PET}\le N_A^{\max} \tag{9}$$

where $N_A^{\min}$ and $N_A^{\max}$ are the minimum and maximum number of PETs that are planned to be installed in the power system.

The lower-stage optimization performs the power regulation of PET and PV inverters under the configuration parameters given in the upper-stage algorithm. Accordingly, the lower-stage optimization is formulated as:

$$\min LP\left(S_{Vi}^{m}(t),P_{i,PET}(t)\,|_{P_{i,PET}^{\max}(t),LC_{i,PET}}\right)=\sum_{i=1}^{n}\rho_{el}(t)\left(P_{Ld}(t)-P_{Vi}(t)+P_{Ls}(t)\right)+\rho_{V}(t)P_{Vi}(t) \tag{10}$$

where $S_{Vi}^{m}(t),P_{i,PET}(t)\,|_{P_{i,PET}^{\max}(t),LC_{i,PET}}$ represents the decision variables in the lower stage which is solved at each time interval since the power regulation is time-independent.

$$Q_{i,k}^{PV}(t)^2\le S_{R,k}^2-\left(P_{i,k}^{PV}(t)+P_{i,k}^{LS}\right)^2 \tag{11}$$

where $S_{R,k}$ is the rated capacity of PV inverter; $P_{i,k}^{PV}(t)$ and $P_{i,k}^{PV}(t)$ are the active and reactive power of the PV unit *k*; $\tan\theta$ is the limit put on the power factor of devices connected to the distribution feeders; $P_{i,k}^{LS}$ is the power loss of the power electronic interface.

The other commonly used constraints that describe the limits on the power regulation of PV and power electronic converters can be found in previous research work [11-14].

4. Simulation results

4.1. Case study

A 33-bus distribution network is adopted for simulation studies [15]. In order to analyze the effects of large-scale penetration of PV generation, PV units are installed onto four buses in the network, as shown in Fig. 2. For time-series simulation, the active and reactive loads are calculated by multiplying the coefficient that reflects the daily load curve as shown in Fig. 3. The original load is equivalent to the load level indicated by coefficient 0.85. The two-tariff pricing is adopted for daily electric energy price including two main periods. The candidate locations for PET configuration are those buses with installed PV generation and DC load such as charging infrastructure for electric vehicles. It is assumed that two traditional transformers are to be replaced by PETs considering the budget for upgrading the distribution grid.

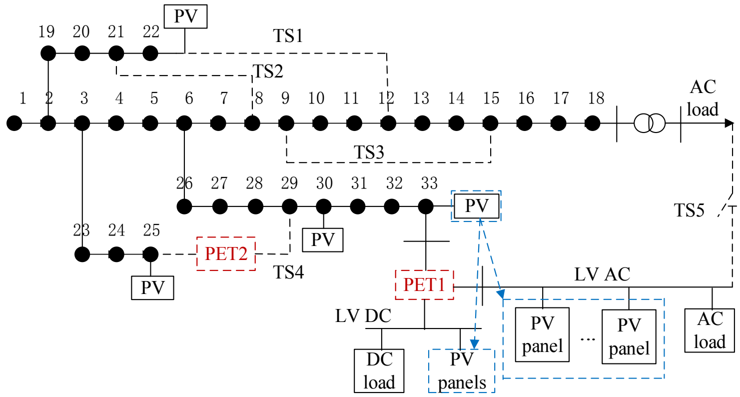

Fig 3. 33-bus distribution network with PV integration and updated PET bus

Table 1. Simulation parameters.

Parameter name	Parameter value	Parameter name	Parameter value	Parameter name	Parameter value
PV node 22	0.5MW	PV node 33	1.5MW	Electricity price	0.8 CNY/kwh
PV node 25	1.5MW	TS1	1.0MW	f1	0.3
PV node 30	1.0MW	TS2	1.0MW	f2	0.08MW

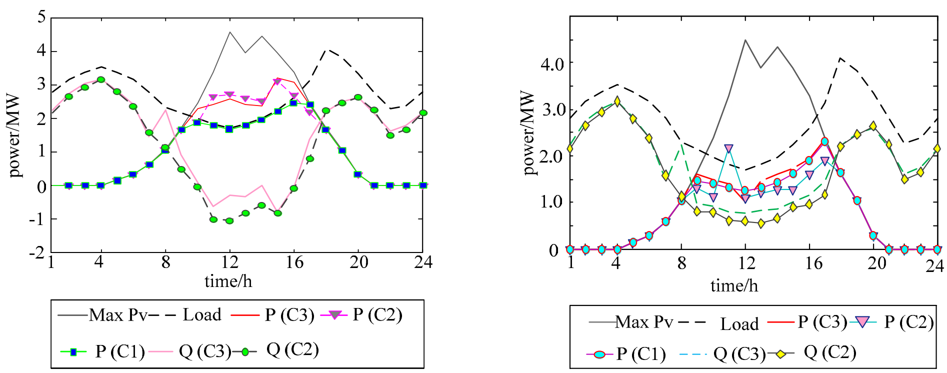

Fig. 4. Daily power profiles of load and PV generation in the scheme 1 and scheme 2

In this paper, acceptable range of voltage domain is considered between 0.95 and 1.05 p.u. for the studied test system. The voltage limit is rigidly enforced which means the excessive PV generation in the midday sun must be curtailed and thus affecting the utilization rate of PV generation. Three cases are compared for simulations conducted in this investigation corresponding to different control strategies of PV inverters, along with the updated PET at two buses:

Case 0: The case without PV integration, as an extra reference case.

Case 1: The case with active power control of PV inverters, in which only the active power of PV inverters is adjusted to comply with the constraints of power system operation.

Case 2: The case with active power and reactive power control of PV inverters, in which both active and reactive power are adjusted subject to the operating constraints of PV inverter.

Case 3: The case with power regulation of PV inverters in cooperation with PET configuration.

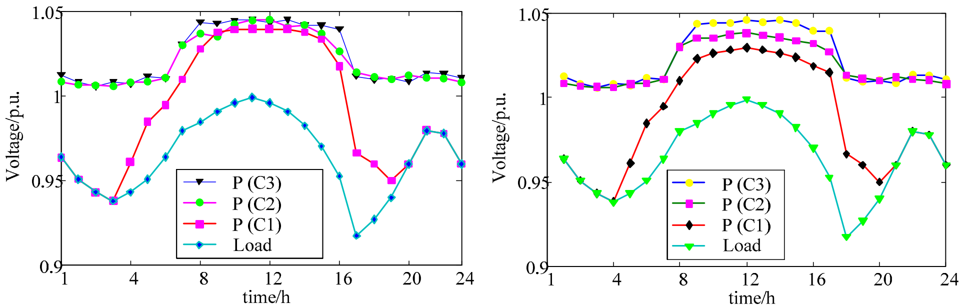

Fig. 5. Daily voltage profiles in scheme 1 and scheme 2 for different cases

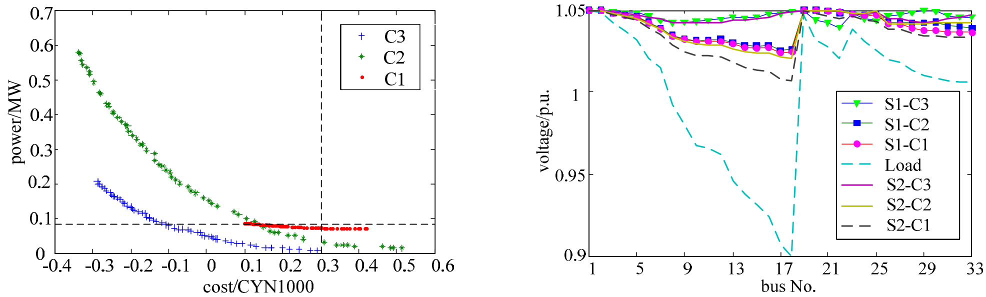

Fig. 6. Pareto front of different cases and the voltage of 33-bus distribution grid in different scenarios

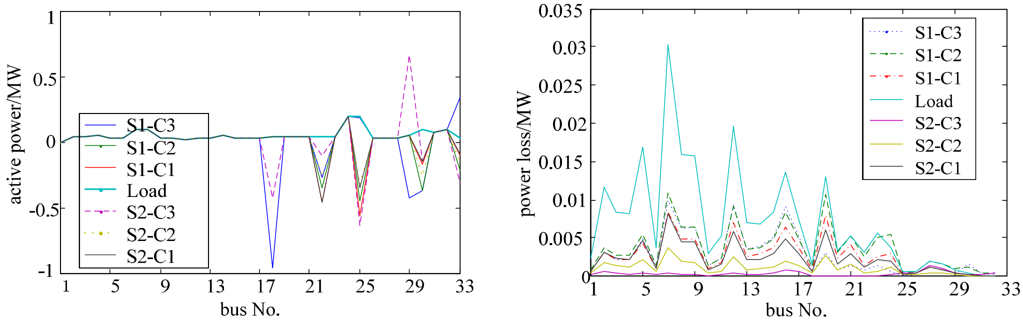

Fig. 7. Active power and power losses of the 33-bus distribution grid in different scenarios

4.2. Result and discussion

The load profile and PV generation profile are given in Fig. 4 based on the optimization solutions. Two schemes are selected to compare the results according to different objectives set in the NSGA-II optimization problem. Scheme 1 (S1) represents the set of control variables resulting in lower cost while scheme 2 (S2) represents control variables resulting in lower power losses. As shown in Fig. 3 and Fig. 4, the voltage can be limit within the regulatory standard in both schemes and the curtailed PV generation can be reduced in scheme 1. The curtailed PV generation can be further reduce by introducing PETs based on Fig. 3. Consequently, the total power losses can be reduced by applying reactive power regulation in the same scheme which can be seen in Fig. 4.

The Pareto front can be depicted after the NSGA-II optimization. The two schemes in different cases are chosen based on the same first or second objective function as shown in Fig. 5. The PET-aided control strategy for large-scale PV integration gives the best fitness function where both objectives can reach better lower values. In Fig. 6, the active power at each bus shows the absorption rate of PV especially at the time interval of maximum PV generation can be significantly improved by introducing PETs and the power losses can be reduced by flexibly adjust the active and reactive power of PV inverters.

5. Conclusion

Proper reformation of the distribution grid with PETs can play a important role in integrating large-scale renewable energy resources such as photovoltaic and maximizing the economic and environmental benefits. In the paper, the optimal configuration of updated PET is coordinated with the optimal dispatching of photovoltaic generation units. Two-stage optimization model is derived to solve the complex multi-objective minimization of cost and power losses in a test distribution network by regulating the PET and active and reactive power of PV inverters. Finally, the synergy effects of the proposed PET-aided RES optimal scheduling mechanism is evaluated in terms of RES penetration level, voltage profiles, network losses through simulation of a MV residential distribution network. Furthermore, the benefits of the proposed optimal scheduling for integrating large-scale RES into the power grid can be effectively communicated to practicing engineers and applied to demonstration project in real-world setups.

Acknowledgements

This work was partially supported by the National Key R&D Program of China (2016YFB0900400), and the National Nature Science Foundation of China (51707130).

References

[1] M. Bianchi, L. Branchini, C. Ferrari, F. Melino, “Optimal sizing of grid-independent hybrid photovoltaic–battery power systems for household sector”, Applied Energy, vol. 136, pp. 805-816, 2014.
[2] Nasim Sahraei, Erin E. Looney, Sterling M. Watson, Ian Marius Peters, Tonio Buonassisi, “Adaptive power consumption improves the reliability of solar-powered devices for internet of things”, Applied Energy, vol. 224, pp. 322-329, 2018.
[3] Myungchin Kim, Sungwoo Bae, “Decentralized control of a scalable photovoltaic (PV)-battery hybrid power system”, Applied Energy, volume 188, pp. 444-455, 2017.
[4] Heydari and A. Y. Varjani, "Combined modified P&O algorithm with improved direct power control method applied to single-stage three-phase grid-connected PV system," 2018 9th Annual Power Electronics, Drives Systems and Technologies Conference (PEDSTC), Tehran, 2018, pp. 347-351.
[5] J. P. Contreras and J. M. Ramirez, "Multi-Fed Power Electronic Transformer for Use in Modern Distribution Systems," in IEEE Transactions on Smart Grid, vol. 5, no. 3, pp. 1532-1541, May 2014.
[6] F. Shahnia and A. Ghosh, "Coupling of neighbouring low voltage residential distribution feeders for voltage profile improvement using power electronics converters," in IET Generation, Transmission & Distribution, vol. 10, no. 2, pp. 535-547, 2016.
[7] M. M. Hasaneen, M. A. L. Badr and A. M. Atallah, "Control of active/reactive power and low-voltage ride through for 40 kW three-phase grid-connected single-stage PV system," in CIRED - Open Access Proceedings Journal, vol. 2017, no. 1, pp. 1655-1659, 2017.
[8] J. D. Watson, N. R. Watson and B. Das, "Effectiveness of power electronic voltage regulators in the distribution network," IET Generation, Transmission & Distribution, vol. 10, no. 15, pp. 3816-3823, 2016.
[9] M. Florkowski, J. Furgał, M. Kuniewski, "Propagation of overvoltages in distribution transformers with silicon steel and amorphous cores", IET Gener. Transm. Distrib., vol. 9, no. 16, pp. 2736-2742, 2015.
[10] Chuang Liu, Xuejiao Li, Yuemei Zhi, Guowei Cai, “New breed of solid-state transformer mainly combing hybrid cascaded multilevel converter with resonant DC-DC converters”, Applied Energy, vol. 210, pp. 724-736,2018.
[11] Y. Ru, J. Kleissl, S. Martinez, "Size determination for grid-connected photovoltaic systems", IEEE Trans. Sustain. Energy, vol. 4, no. 1, pp. 68-81, Jan. 2013.
[12] I.-K. Song, W.-W. Jung, J.-Y. Kim, S.-Y. Yun, J.-H. Choi, S.-J. Ahn, "Operation schemes of smart distribution networks with distributed energy resources for loss reduction and service restoration", IEEE Trans. Smart Grid, vol. 1, no. 2, pp. 367-374, Mar. 2013.
[13] Z. Ziadi, S. Taira, M. Oshiro and T. Funabashi, "Optimal Power Scheduling for Smart Grids Considering Controllable Loads and High Penetration of Photovoltaic Generation," in IEEE Transactions on Smart Grid, vol. 5, no. 5, pp. 2350-2359, Sept. 2014.
[14] Fang-Fang Li, Jun Qiu, “Multi-objective optimization for integrated hydro–photovoltaic power system”, Applied Energy, vol. 167, pp. 377-384, 2016.
[15] Savier J S, Das D. “Impact of Network Reconfiguration on Loss Allocation of Radial Distribution Systems”, IEEE Transactions on Power Delivery, 2007, 22(4):2473-2480